J Mater Sci (2010) 45:5581–5590
DOI 10.1007/s10853-010-4620-3

Safety evaluation of composites with a wrinkled fabric preform under bending

Thanh Trung Do · Dong-Joo Lee

Received: 18 February 2010 / Accepted: 13 May 2010 / Published online: 29 May 2010

Abstract Wrinkled fabrics in the preform exert significant influence on the qualities of resin transfer molded composites (RTMCs). The bending properties of composites with wrinkled fabrics were studied using several wrinkled models with different wrinkled lengths and numbers of fabric plies, as well as three different matrices and four different loading rates. It was found that the measured bending properties with a strong matrix are less sensitive to wrinkling than those with a weak matrix. The bending moduli of a composite with wrinkled fabric preform are larger than those of a composite with a non-wrinkled fabric preform even under the same effective fiber volume fraction (V_f') when the composite is loaded in the middle of the wrinkled region. The bending strengths of the wrinkled models are lower in low V_f' and higher in high V_f' than those of a perfect sample. Also, the bending strengths indicate two failure mechanisms as a function of the ratio of the wrinkled length to the span length (L_W/L). Based on the experimental data, safe strength conditions of the wrinkled models that are better than those of a perfect sample are suggested under three-point bending.

Introduction

Resin transfer molding has been used to produce high-performance polymer composites for structural components in the aerospace, sports, and automobile sectors [1–3]. There are many advantages in using resin transfer molded composites (RTMCs) over traditional composite processing techniques, such as the filament winding and compression molding of prepreg tape laminates as highly complex structures, low temperature and pressure requirements, and short cycle times. Also, RTMCs possess some unavoidable disadvantages due to the deformation of fabrics during preform loading and/or the void content during injection and curing processes. These drawbacks can be a source of both initial micro-cracks and final failure. However, some cases of deformed preforms, such as wrinkled and overlapped fabrics, can be the result of stacking sequences and material properties as well as of in-plane loading that depends on the loading conditions [4–6]. In those cases, the deformed preforms exert considerable influence on mechanical properties and failure modes of RTMCs.

Void problems can exist in finished composites due to the void content of resin prior to injection and the extent of void formation as well as growth during the mold filling and cure processes. Varna et al. [7] studied the influence of voids on the global mechanical behavior of laminates in transverse tensile loading and reported that the laminates have different types of void and void content. Low void-content specimens not only had high strength but also showed brittle behavior with low strain to failure. High void-content specimens showed linear stress/strain behavior at the early stage of the deformation process. Only large and well-defined transverse cracks formed in low void-content laminates before final failure. Multiple transverse cracks with irregular shapes as well as numerous smaller cracks formed in the high void-content laminates. The irregularity of these cracks resulted in lower stress concentrations and stress levels in the weft fibers. In addition, discontinuous fibers can occur during the preform loading and thermoforming processes in the closed mold.

T. T. Do · D.-J. Lee (✉)
School of Mechanical Engineering, Yeungnam University, 214-1, Dae-dong, Gyeongsan, Gyeongbuk 712-749, Korea
e-mail: djlee@yu.ac.kr

T. T. Do
e-mail: thanhtrungspkt@yahoo.com

The damage to composite materials due to the discontinuous fibers involves several failure modes such as matrix micro-cracking, interfacial debonding, and fiber pull-out [8–11]. This is due to the efficiency of the fiber/matrix load transfer mechanisms and the stress concentration at the fiber ends in composites. Several studies have focused on the influence of composites with discontinuous fabrics on the mechanical behavior and failure mechanisms. For instance, Holmberg and Berglund [12] studied the problems of the fabric preform of U-beams. They reported that the reinforcement easily led to discontinuity in the fabric during preforming and/or mold closure. The discontinuity in the fabric preform caused the problem of void content in the finished composites. Also, the failure mechanisms of composites with either continuous or discontinuous fibers in the preform varied across the failure modes and was affected by the material stiffness, geometrical preform, processing technique, loading type, etc. Sreekumar et al. [13] reported that the failures of laminated composites encompass fiber breakage, fiber pull-out, and fibrillation, which have different failure locations as functions of the fiber length and fiber volume fraction. The failures transpired at the highest stress concentrations, which were related to the mechanical properties of the composites. In general, the mechanical qualities of RTMCs depend on several parameters such as materials, the preform architecture, and loading conditions; therefore, further research is necessary.

Recently, we developed a simple analytical model based on the measured bending properties and failure mechanisms of composites with wrinkled fabric preforms by comparison with the results of composites with non-wrinkled preforms as functions of the fiber volume fraction and other parameters [14].

The main objectives of this research are to provide the "safe bending strength conditions" of composites with wrinkled fabric preforms by examining the influence of fabric preforms with varying wrinkled lengths and fabric ply numbers as well as three matrices and four loading rates under three-point bending. The failure modes related to the bending strength depend not only on the wrinkled length but also on the material properties and conditions of testing. Hence, the "safe bending strength conditions" of composites need to be considered and proposed for designing composite products with wrinkled fabric under the bending model.

Experimental

Materials

The E-glass plain woven fabric, K618, which has the same properties in both the warp and weft directions, was obtained from Hankuk Fibers Co. and used as the reinforcement. Three polyester resins, viz., R409, R235, and SR825, which were obtained from Sewon Chemical Co. in Korea, were used as the polymer matrix. For the curing process at a room temperature of 25 °C, the hardener material, Luperox DDM from Seki Arkema Co., was mixed with the resins in a weight ratio of 1:120. Moreover, the accelerator agent of P-VN from Sewon Chemical Co. was also added to the previous mixture of the polyester, SR825, and hardener, DDM. Table 1 presents the basic physical and mechanical properties of the materials of the composites.

Laminate fabrication

The laminate composites were fabricated by a resin transfer molding process whereby the fabric preform was first placed into a rectangular mold of 200 mm × 300 mm. Then, the mixed polyester-hardener in the form of a liquid was injected into the closed mold through the inlet while the remaining air escaped from the mold through the vents. Fiber-reinforced resin materialized inside the mold at room

Table 1 Basic physical and mechanical properties of the resin and fabric materials

Type	Density (g/cm^3)	Viscosity (Poise/25 °C)	Curing time at 25 °C (min)	Bending strength (MPa)	Bending modulus (GPa)
Polyester resin (after curing)					
R409	1.12	1.17	7	45	2.3
R235	1.05	1.15	7	48	3
SR825	1.05	1.15	5	51	3.8

Count (Yarns/in.)		Density (g/cm^3)	Thickness (mm)	Bending strength (GPa)	Bending modulus (GPa)
Warp	Weft				
E-glass plain woven fabric (K618)					
18	18	2.54	0.18	3.4	70

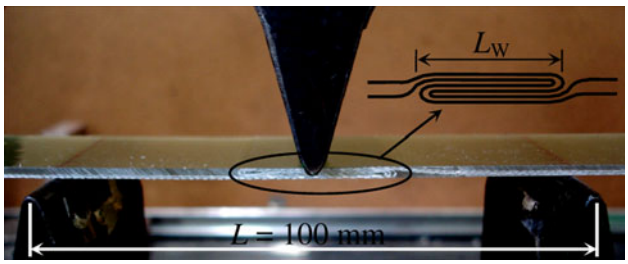

Fig. 1 Set-up of a three-point bending specimen with the wrinkled model

temperature and was fully cured after 2 h. Then, the finished composite was demolded [2, 15, 16]. The laminate composites had uniform thicknesses, $t = 2.5$ mm for K618/R409 and $t = 2.1$ mm for K618/R235 and K618/SR825. In this study, the structures of the fabric preform have two models including the non-wrinkled and wrinkled models, which have various numbers of fabric plies within the same warp and weft directions in the preform. The wrinkled preform was fabricated during the loading process from the plain woven fabrics, as shown in Fig. 1, and had varying wrinkled length as the ratio of the wrinkled length to the span length, L_W/L, ranged from 0.1 to 0.9. To make the wrinkled preform with various wrinkled lengths, the plain woven fabrics with extra length for wrinkling length were prepared. Then, the fabric plies were laid into the mold by hand to form wrinkled fabrics. A number of fabric plies in the wrinkled models involved 1, 2, 3, and 4 plies. The detailed conditions are the same as those described in previous paper [14].

Specimens and testing

The specimens were cut from the original laminates by a circular saw machine along the reinforcing fiber direction with a length of 190 mm and width of 33.3 mm. The wrinkled region was located at the middle section of the specimens. The three-point bending tests, which had a span length of $L = 100$ mm, were performed using a Shimazu testing machine at a room temperature of 25 °C and relative humidity of 50%. All tests were done with the radius of 2 mm for the loading head and supports. According to Ref. [17], the radii of the loading head and supports could influence the mechanical properties and should be chosen to reduce the excessive indentation or failure due to stress concentration directly under the loading head and supports. Also, the arc of the loading head and supports in contact with the specimen would be sufficiently large to prevent contact of the specimen with the sides of the head and supports. Based on the preliminary tests with other sizes, 2 mm radius seems to be suitable since 1 mm for stress concentration and 3 mm for contact and sliding problems. Typically, the bending load was applied at the middle of the span, as shown in Fig. 1, with a loading rate of 5 mm/min and recorded with the deflection of the beam [17]. Moreover, different loading rates (3, 15, and 50 mm/min) were also examined to enhance the understanding of their effects on the bending strength. At least three samples were prepared for each group from which the mean values were reported.

Results and discussion

Influence of the matrix on the mechanical properties

For the three-point bending mode with a thin thickness of the laminated composites, both the normal stress and shear stress should be present throughout the beam span. The total deflection (δ) at the mid-point of the beam with normal and shear factors is considered as follows [18]:

$$\delta = \frac{PL^3}{4Ebt^3} + \frac{3PL}{10Gbt} \tag{1}$$

where $G = \frac{E}{2(1+v)}$ and v is the Poisson's ratio.

In Eq. 1, P is the applied load, L is the span length, b and t are the width and thickness of the specimen, respectively, and E and G are the normal and shear moduli, respectively. Strictly speaking, this equation can be used for an isotropic material and also used with caution for a material with "fiber" symmetry as in woven or cross-plied fabrics at fiber reinforcements of 0° and 90°.

Then, the bending modulus and strength of the specimen can be given as follows:

$$E = \frac{PL^3}{4\delta bt^3}\left(1 + \frac{12}{5}(1+v)\left(\frac{t}{L}\right)^2\right) \tag{2}$$

$$\sigma_{\max} = \frac{3P_{\max}L}{2bt^2}\left[1 + 6\left(\frac{\delta^*}{L}\right)^2 - 4\left(\frac{t}{L}\right)\left(\frac{\delta^*}{L}\right)\right] \tag{3}$$

In Eq. 3, δ^* is the deflection at the middle of the beam corresponding to the maximum load of $P_{\max}$.

Figure 2 depicts the load–displacement curves of the K618/R409 composite with several fabric plies. First, there was a linear region where the composite was elastic for representing the stiffness of the composite. Then, the bending load increased monotonically with the deflection and obtained its maximum value when the fibers achieved their potential strengths that related to the failure modes. Thus, from those load–displacement curves using Eqs. 2 and 3, respectively, the bending modulus and bending strength of the composites could be determined for various fiber volume fractions as well as reinforcing elements. At the maximum applied load, those curves observed with different failure modes and propagation processes that

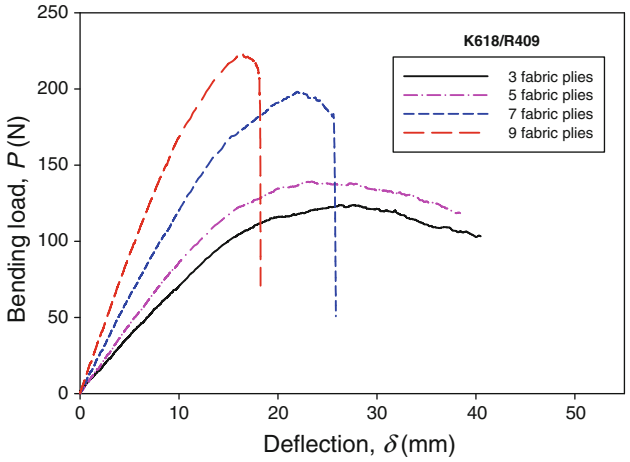

Fig. 2 Load–deflection curves of the K618/R409 composite with a non-wrinkled preform

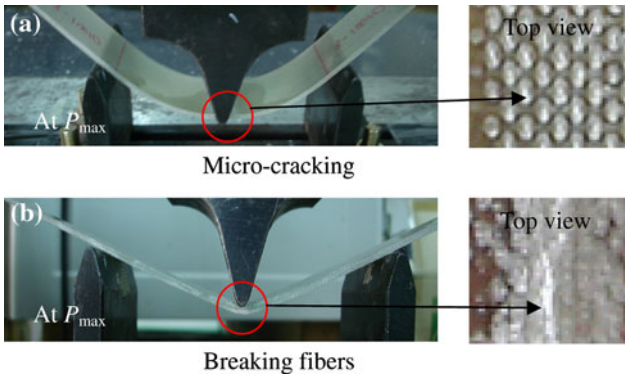

Fig. 3 Failure modes of the K618/R409 composite with a non-wrinkled preform

depended on number of fabric plies. When the number of fabric plies in the composites was low, i.e., three or five fabric plies, the micro-cracking of the fiber/matrix interface occurred initially on the compression side around the loading head at the maximum applied load and then enlarged with the specimen deflection, as shown in Fig. 3a. It can be believed that this phenomenon was due to not only the nature of materials but also the stress concentration influencing from the loading head. However, the failure was due to the breaking fibers on the tension side (Fig. 3b) when the number of fabric plies was high, i.e., seven or nine. Also, the deflection at the mid-span of the beam decreased with increasing number of fabric plies in the preform, which was expected for the same thickness. It is clear that a composite with a low fiber volume fraction is more flexible than that with a high fiber volume fraction, which affects the stiffness and strength of the laminated composites [9, 13, 19].

Also, the physical and mechanical properties of materials including the matrix viscosity, element reinforcement, and geometrically discontinued fabrics, can impact the quality of RTMCs [8, 20, 21]. To confirm the influence of the matrices, the bending modulus (E) and bending strength (σ_{max}) of the composites with three different matrices (K618/R409, K618/R235, and K618/SR825) were examined and shown in Fig. 4. Those composites were fabricated from the same fiber material (K618) as the non-wrinkled preform. It can be seen that the experimentally measured results increased with the number of fabric plies (Fig. 4a) as well as the effective fiber volume fraction (V_f') (Fig. 4b). V_f' was calculated based on the respective densities of the matrix, fiber, and composite and assumed to be 50% of that of the measured fibers in the fabric preform; this was due to the load carrying fibers owing to the nature of the woven fabric, K618, which has "fiber" symmetry when cross-plied at the 0° and 90° directions. For a given V_f' of 6%, the differences in the bending modulus of K618/SR825 relative to those of K618/R409 and K618/R235 were approximately 1.9 GPa and 0.9 GPa, respectively, and the differences in the bending strength were approximately 18 MPa and 11 MPa, respectively. For a given V_f' of 14%, the differences in the bending modulus of K618/SR825 relative to those of K618/R409 and K618/R235 were about 3.6 GPa and 1.2 GPa, and the differences in the

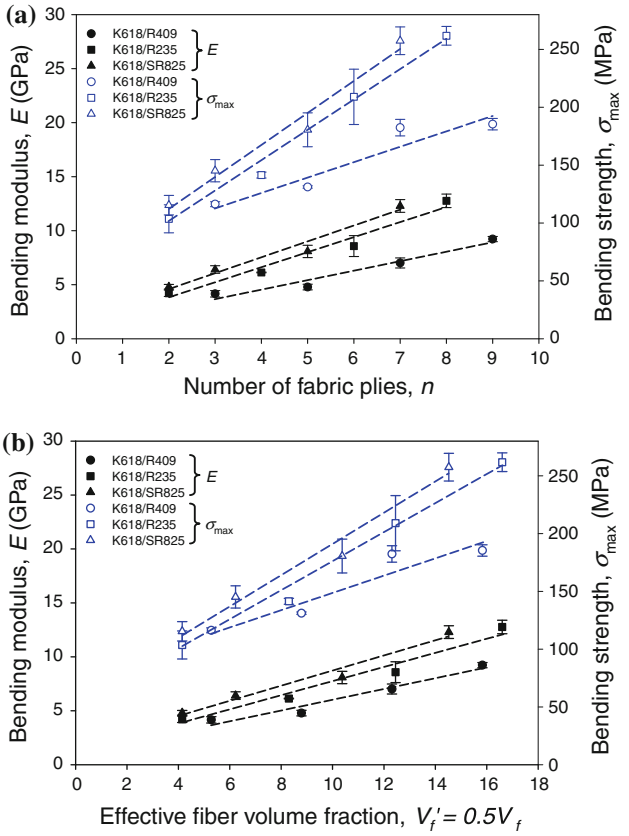

Fig. 4 Bending moduli and bending strengths of composites with non-wrinkled preforms

bending strength were about 75 MPa and 20 MPa, respectively. The extent of the differences depended on both the matrix and the fiber volume fraction that indicated the fiber bridging matrix and stress transfer under bending [20, 22]. The mechanical properties of composites were found to depend on the stacking sequence and matrix system. For composites with the small number of plies or low effective fiber volume fraction, the loading capacity was strongly dependent on the interlaminar shear stress of the matrix that occurred in sub-surface plies. However, with the larger number of plies or higher effective fiber volume fraction, the load carrying fibers were dependent not only on the potential strengths of materials but also the fiber bridging matrix, which related to the resin viscosity and permeability in RTMCs. Also, under a matrix with low viscosity, it was easy to thoroughly wet the preform with a reduction in the void content and enhance the matrix for fiber interaction in RTMCs [23, 24]. In general, as a function of V_f', the bending modulus and bending strength of the composite with a high stiffness matrix increase rapidly and are larger than those of a composite with a low stiffness matrix. It is clear that the influence of the matrix on the mechanical properties is small when the fiber volume fraction is small, but becomes larger when the fiber volume fraction increases.

Influence of the wrinkled preform with different matrices on the mechanical properties

Figure 5 depicts the variation with the effective fiber volume fraction (V_f') of the bending modulus of the K618/SR825 composite, which is fabricated from either non-wrinkled or wrinkled preforms (with varying number of plies). For wrinkled preform models, a number of fabric

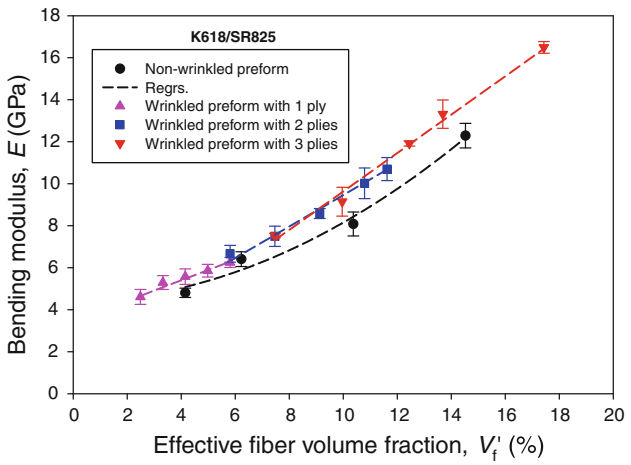

Fig. 5 Variation of the bending modulus of the K618/SR825 composite with the effective fiber volume fraction for different wrinkled lengths

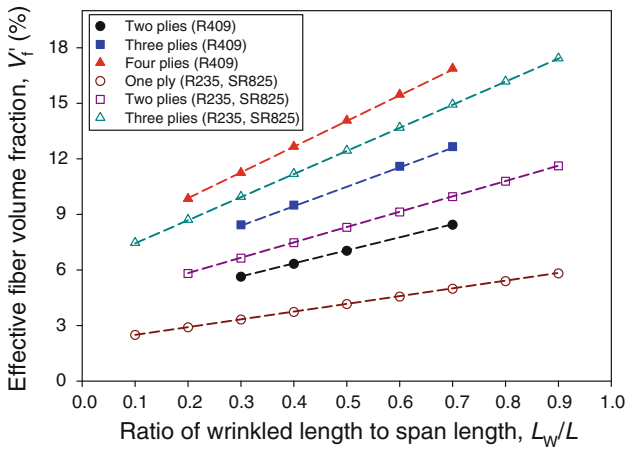

Fig. 6 Effective fiber volume fraction (V_f') versus the ratio of wrinkled length to span length (L_W/L)

plies in the wrinkled region were three times more than the one in the non-wrinkled region. It led to the effective fiber volume fraction (V_f') in the wrinkled region of the beam which was larger than that in the non-wrinkled region when $L_W/L > 0.25$ as well as the V_f' in the wrinkled region was smaller than the one in the non-wrinkled region when $L_W/L < 0.25$. Therefore, the V_f' used throughout the beam span of the wrinkled models was averaged from the wrinkled and non-wrinkled regions. The V_f' increased with increasing L_W/L as shown in Fig. 6. Due to the nature of the geometrical preform and loading type, the fiber concentration occurred at the wrinkled region and affected the carrying load of the beam under bending. Thus, the bending modulus of the wrinkled models was almost larger than that of the non-wrinkled preform as a function of V_f'. In addition, the results of the wrinkled models were almost the same for a given V_f' even when the number of wrinkled fabric plies and wrinkled lengths differed in the preform. It is clear that the wrinkled models can be expected in some cases for improving the bending modulus and have a large value with a high fiber volume fraction.

To examine the influence of the stiffness matrix materials on the bending modulus of composites with wrinkled preforms, comparisons between the non-wrinkled and wrinkled models for three different matrices were done as shown in Fig. 7. ΔE is the difference in the bending moduli of composites with wrinkled and non-wrinkled models as a function of the effective fiber volume fraction regardless of the number of fabric plies in the preform. The results indicate that the composite with a low stiffness matrix (K618/R409) has larger ΔE and is more affected than the composite with a high stiffness matrix (K618/SR825). The physical and mechanical properties of matrices should be similar to both properties of fiber/matrix interface and the delaminated matrix. It led to a difference in the stress

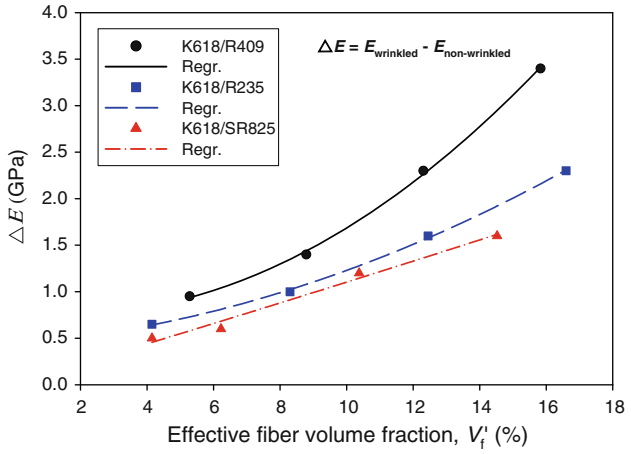

Fig. 7 Difference in the bending modulus between the non-wrinkled and wrinkled models for three different matrices

and yield cross-linking of the composites with three different matrices. Also, the influence of segregation depended on the geometrical structure of the fabric preform and the fiber/matrix interface [9, 21, 25]. The difference in the bending moduli of composites with non-wrinkled and wrinkled models increased with increasing V_f'. It is clear that composites with high fiber volume fractions are more sensitive to wrinkling.

The variation with the fiber volume fraction of the bending strength of composites with the wrinkled preform for K618/R409, K618/R235, and K618/SR825 corresponding to various wrinkled lengths manifested two phases, as shown in Fig. 8a–c, respectively. This phenomenon was due to the efficiency of the fiber/matrix load transfer mechanisms and the stress concentrations at the wrinkling ends in the preform of the composites. The bending strength was controlled by the interfacial bonding strength between the fiber and matrix for the first phase when the wrinkled length (L_W) was smaller than the critical wrinkled length (L_{CW}). However, it was controlled by the potential strength of the fibers for the second phase when $L_W > L_{CW}$. The experimentally measured results of the second phase increased and had a greater slope than those of the first phase. The separation of the two phases with the increase in the critical wrinkled length of L_{CW}, as shown in Fig. 9, indicates that a composite with a strong matrix has a short L_{CW}. Moreover, differences in the bending strengths of the composites that were fabricated by the three different matrices were small when the wrinkled length was small. But they became larger when the wrinkled length increased. It is clear that the bending strength of the composite depends not only on the matrix but also on the geometrical preform as the wrinkled pattern.

The failure mode and propagation process until ultimate ply failure (that is related to the maximum load) depended

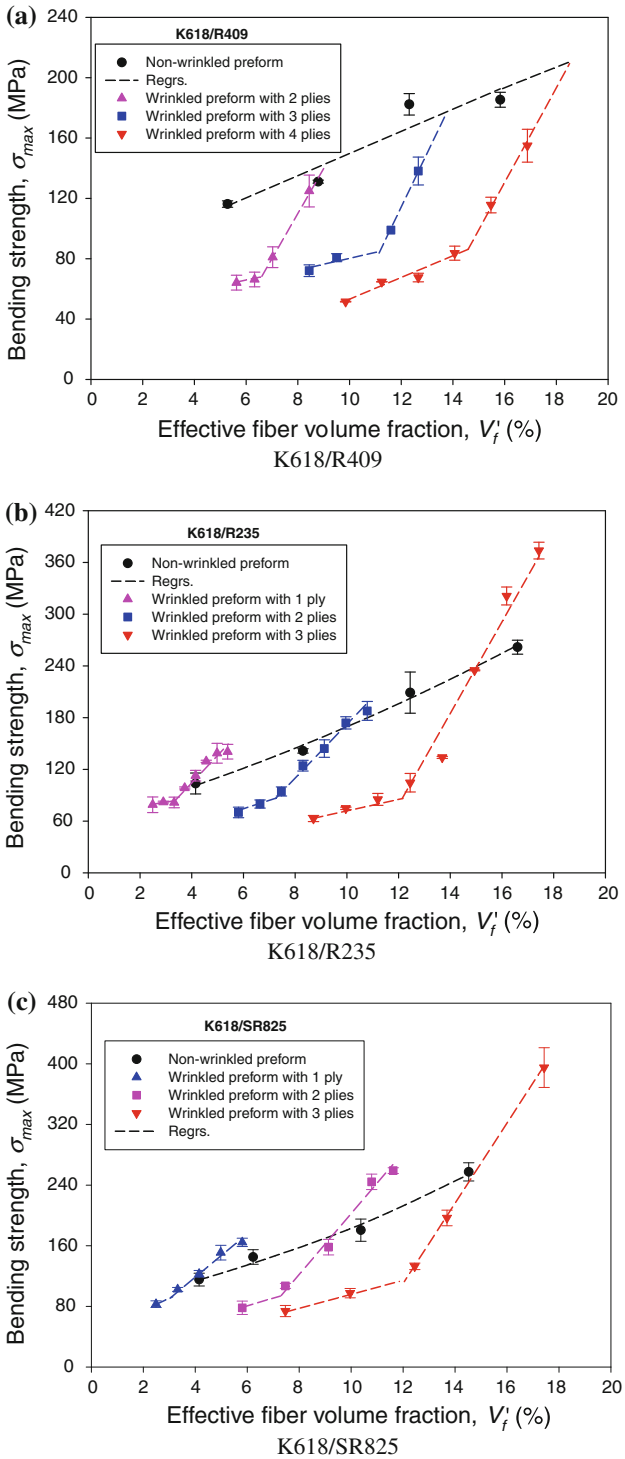

Fig. 8 Experimentally measured bending strengths of composites with non-wrinkled and wrinkled models

on the wrinkled length and number of fabric plies. When $L_W < L_{CW}$, the interfacial failure was the dominating failure mechanism [8, 25, 26]. The initial cracks occurred at the wrinkling ends, which had the load-transfer and stress concentrations because the wrinkled fabrics were

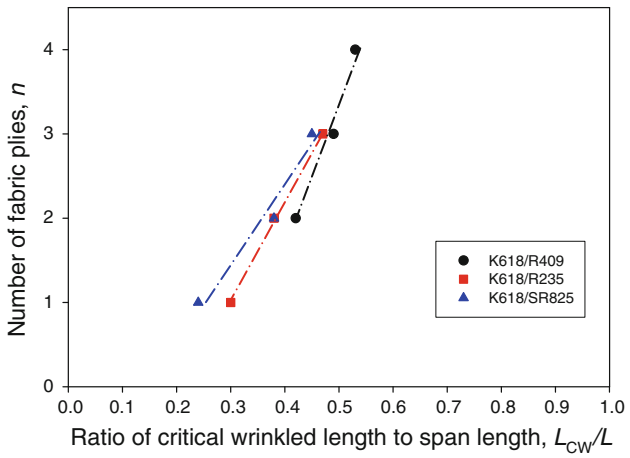

Fig. 9 The ratio of critical wrinkled length (L_{CW}) depending on the number of fabric plies

assumed to be discontinuous fibers, and led to reductions in the strength and life due to the growth in damage around these stress concentrations. Further loading caused a weak fiber/matrix bond so that as the micro-cracks reached the interface, they got deflected along the interface rather than pass straight through the fibers. Then, the matrix bridges failed, and the interfacial cracks grew and connected with the macroscopic cracks. Finally, the fiber and matrix of the wrinkled region would result in debonding as the opening failure mode, as shown in Fig. 10a. On the other hand, upon further increment in the wrinkled length within the range, $L_W > L_{CW}$, failure was due to the buckling and/or micro-crack fibers that occurred at the wrinkling ends or the location of application of the loading with high stress concentrations [9, 12], as shown in Fig. 10b, c. The fibers could achieve their potential strength and the composite failure was controlled by the fibers. Thus, from the viewpoint of the failure mode, composites with wrinkled fabric preforms always have two failure mechanisms that depend on the wrinkled length or fiber volume fraction. The

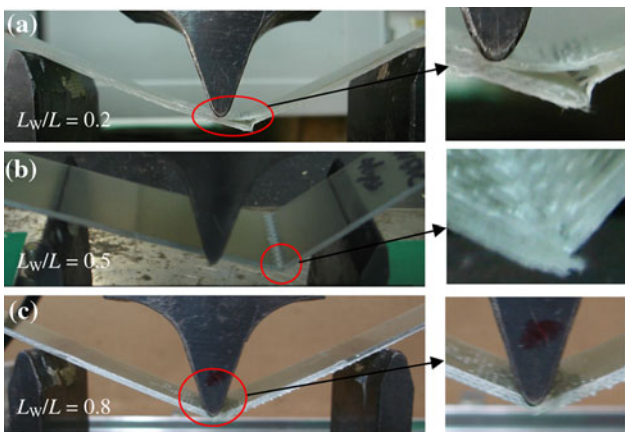

Fig. 10 Failure mechanisms of composites with wrinkled preforms

bending failure that is related to the bending strength of the composite is controlled by the toughness of the matrix for the first phase ($L_W < L_{CW}$) and the potential strength of fibers for the second phase ($L_W > L_{CW}$). Also, the bending strength of composites with wrinkled preforms for the second phase increases more quickly than that of the first phase as a function of the fiber volume fraction.

Safety model for composites with wrinkled fabrics

A comparison of composites with non-wrinkled and wrinkled models with respect to the bending strength as a function of the fiber volume fraction, which are expected for various numbers of fabric plies and wrinkled lengths, indicates that the results of the wrinkled model could be larger than those of the non-wrinkled model when the wrinkled length (L_W) was large enough, i.e., $L_W > L_{SW}$, where L_{SW} was the safe wrinkled length. Improved properties resulted for the composites with wrinkled preforms due to the contribution of the fiber concentration and the realized potential strength of the fibers at the location of the applied loading. To use the safe wrinkled length (L_{SW}) from the experimental data for designing composites, it is necessary to generalize this behavior. If composite products with wrinkled fabric are loaded under bending and over the wrinkled region, the safety of such products can be predicted as a function of the bending modulus (E) and bending strength (σ_{max}) of the composite with a given number of fabric plies (n) or effective fiber volume fraction (V_f'). Thus,

$$n = f(L_{SW}, L, \sigma_{max}, E). \tag{4}$$

Based on this study, the number of fabric plies (n) should be converted to the effective fiber volume fraction (V_f') at the safe wrinkled length (L_{SW}) as follows:

$$V_f' = k\left(\frac{E}{\sigma_{max}}\right)^{0.6} e^{q\left(\frac{L_{SW}}{L}\right)} \tag{5}$$

$$\ln V_f' = \ln k + 0.6 \ln\left(\frac{E}{\sigma_{max}}\right) + q\left(\frac{L_{SW}}{L}\right) \tag{6}$$

In the above equation, k and q are the coefficients that may depend on several conditions such as the geometrical preform, stacking sequence, and matrix system, as well as the type of loading.

For composite products to not fail, σ_C/σ_P should exceed unity, where σ_C is the composite strength and σ_P applies to a perfect or non-wrinkled composite. Then, using the modified rule of mixture [13, 14], we can express this requirement as follows:

$$\sigma_C \geq C_\sigma \sigma_f V_f' + \sigma_m\left(1 - V_f'\right) \tag{7}$$

where σ_f and σ_m are the bending strengths of the fiber and matrix materials, respectively, and C_σ is the fiber efficiency

parameter that indicates a fair correlation between the experimental and predicted results for the bending strength.

Then, by combining Eqs. 5 and 7, we can write

$$\sigma_C \geq \sigma_m + k\left(\frac{E}{\sigma_{max}}\right)^{0.6} e^{q\left(\frac{L_{SW}}{L}\right)}(C_\sigma \sigma_f - \sigma_m) \quad (8)$$

Thus, the design of safe composite products with wrinkled fabric preforms can be predicted for given properties of the matrix, fiber, and composites. In the present study with E-glass woven fabric reinforced composites, the experimentally measured results for the effective fiber volume fraction versus the number of fabric plies and the safe wrinkled length are shown in Figs. 11 and 12, respectively. Based on Eq. 5, the coefficients of k and q were determined and are depicted in Table 2. The value of k was a constant that might depend on the loading type in three-point bending with a loading rate of 5 mm/min. Also, the value of q depended on materials and was larger when the composite with wrinkled preform had a stronger matrix, which was expected for the same fiber material in the preform. By correspondence with different ratios of the bending strength of the matrix to that of the fiber, the value of q can be predicted for other composites as shown in Fig. 13. The fiber efficiency parameter that was predicted from the modified rule of mixture was less than unity (Table 2) because of the quality of permeability with the existing void content and the weak fiber/matrix interface depending on the viscosities of the matrices and the natural woven fabric, as well as the processing method [14]. As expected, the safe wrinkled length also can be predicted from the given properties of materials and the fiber volume fraction, as shown in Fig. 14. This prediction can be used as a design tool in the case of wrinkled fabric composites. In general, Figs. 13 and 14 show the importance of the bending strength of the matrix for the composite with wrinkled fabric especially in the range of $q = 2$ and $q = 5$.

Table 2 Coefficients of k, q, and C_σ for given V_f' at L_{SW}

Composite	L_{SW}	V_f'	k	q	C_σ
K618/R409	0.72	8.58	0.85×10^{-3}	3.55	0.3
	0.78	13.5			
	0.85	18.99			
K618/R235	0.45	3.94	0.85×10^{-3}	4	0.35
	0.65	9.54			
	0.74	15.5			
K618/SR825	0.4	3.73	0.85×10^{-3}	4.4	0.41
	0.62	9.25			
	0.71	15.06			

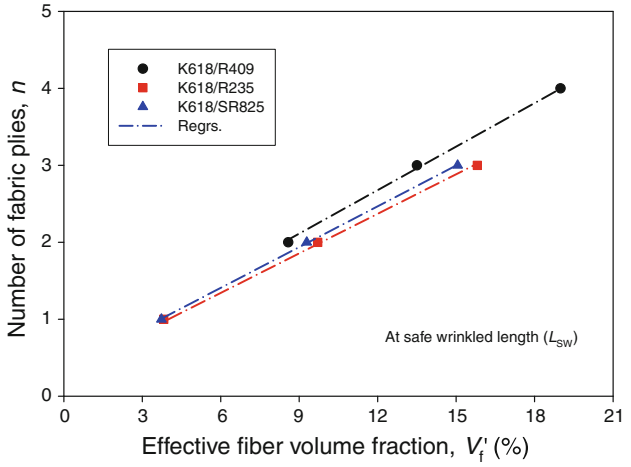

Fig. 11 Effective fiber volume fraction versus the number of fabric plies at the safe wrinkled length

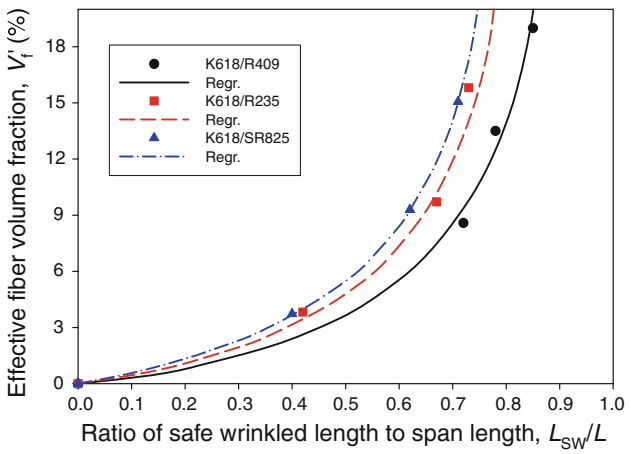

Fig. 12 Effective fiber volume fraction versus the ratio of the safe wrinkled length to the span length

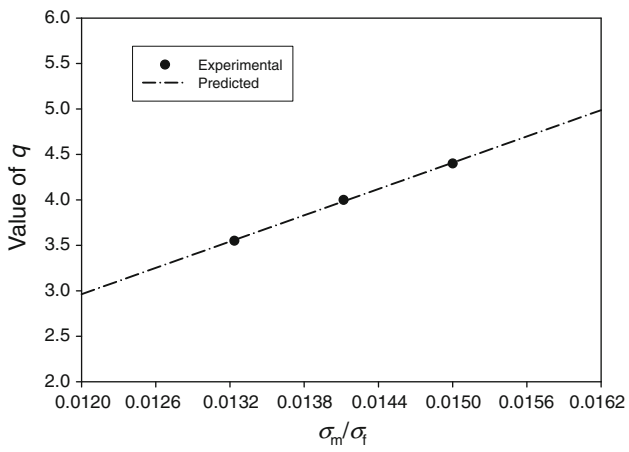

Fig. 13 Prediction of q for given σ_m/σ_f

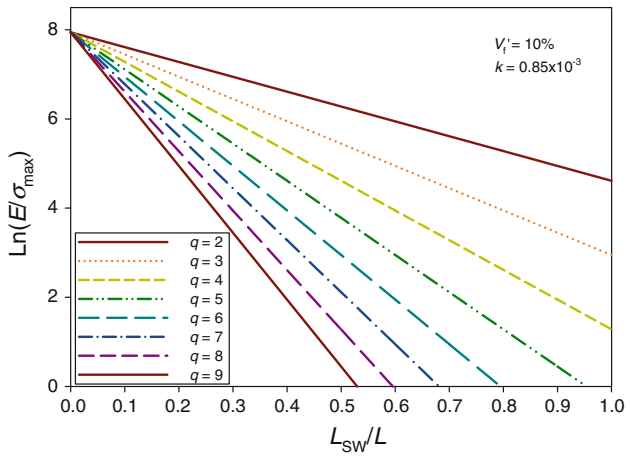

Fig. 14 Prediction of L_{SW}/L for designing composite products

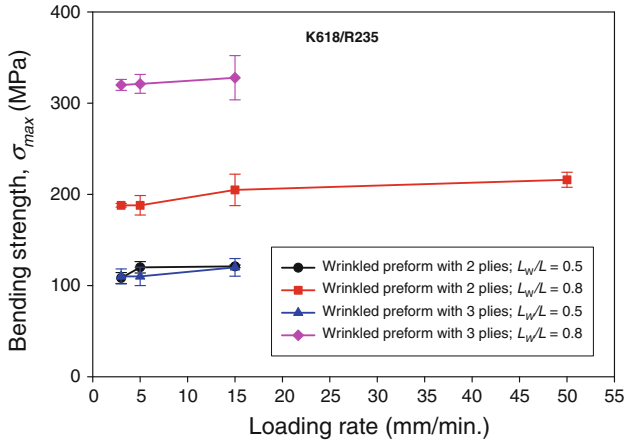

Fig. 15 Bending strength of the K618/R235 composite for various wrinkled lengths and loading rates

Also, the effect of varying the loading rate up to 50 mm/min on the bending strength of the K618/R235 composite with wrinkled models is shown in Fig. 15; this will clarify the impact of the loading rate on the safety evaluation of composite products, which depends on the wrinkled length and/or fiber volume fraction. The experimentally measured results increased slightly with the loading rate, which was expected from the same material and effective fiber volume fraction. The trend in these results is in good agreement with Ref. [27] for fabric-reinforced composites. In other words, the variation in the loading rate leads to a small increase in the bending strength; the change in the value of k is negligible as a function of the tested loading rates under three-point bending. If there are large differences in the bending strength depending on the loading rate, the coefficient, k, can be adjusted. However, the coefficient will not be hugely different since the strengths of normal and wrinkled composites will change similarly for this type of composites.

Conclusions

For composites with non-wrinkled fabric preforms, the experimentally measured results for the bending modulus and bending strength increase with the number of fabric plies or fiber volume fraction. A laminated composite with low fiber volume fraction is more flexible than a composite with high fiber volume fraction. Also, the influence of the matrix on mechanical properties is small when the fiber volume fraction is small, but becomes larger when the fiber volume fraction increases.

For composite with wrinkled fabric preforms, the bending strength and failure can be separated into two phases, which are controlled by the interfacial bonding strength for the first phase when the wrinkled length is small and by the potential strength of the fibers for the second phase when the wrinkled length is larger than the critical wrinkled length. Also, since the bending strength of the second phase increases with a large slope when compared to the first phase, the composite is more sensitive to fibers than to the matrix.

As a function of the fiber volume fraction, the bending modulus of the wrinkled model is always larger than that of the non-wrinkled model. It is clear that the wrinkled model can be expected in some cases for improving the bending modulus of the RTMCs. Also, the bending strength of the wrinkled model can be larger than that of the non-wrinkled model when the wrinkled length, L_W, is larger than, L_{SW}, the safe wrinkled length. The design within the safe wrinkled length ensured the safety of composite products, which can be predicted from the given properties of materials and the fiber volume fraction.

Acknowledgement This research was supported by research grants of Yeungnam University in 2010.

References

1. Potter KD (1999) Composites A 30:619
2. Karlsson KF, Astrom BT (1997) Composites A 28:97
3. Wonderly C, Joachim FG, Cepus E (2005) Composites B 36:417
4. Zhu B, Yu TX, Tao XM (2007) Compos Sci Technol 67:252
5. Potter K, Khan B, Wisnom M, Bell T, Stevens J (2008) Composites A 39:1343
6. Pandey RK, Sun CT (1999) Compos Sci Technol 59:405
7. Varna J, Joffe R, Berglund LA (1995) Compos Sci Technol 59:241
8. Hobbiebrunken T, Hojo M, Adachi T, Jong CD, Fiedler B (2006) Composites A 37:2248
9. Swaminathan G, Shivakumar KN, Sharpe M (2006) Compos Sci Technol 66:1399
10. Friedrich K (1998) J Mater Sci 33:5535. doi:10.1023/A:1004495611093
11. Karbhari VM, Rydin RW (1999) J Mater Sci 34:5641. doi:10.1023/A:1004701604299
12. Holmberg JA, Berglund LA (1997) Composites A 28:513

13. Sreekumar PA, Joseph K, Unnikrishnan G, Thomas S (2007) Compos Sci Technol 67:453
14. Do TT, Lee DJ (2009) J Mater Sci 44:4219. doi:10.1007/s10853-00903492-x
15. Schmachtenberg E, Zur Heide JS, Topker J (2005) Polym Test 24:330
16. Turner DZ, Hjelmstad KD, LaFave JM (2006) Compos Struct 76:352
17. Annual book of ASTM standards (1995) Easton, USA
18. Mallick PK (1998) Fiber-reinforced composites. Marcel Dekker, USA
19. Chen JH, Schulz E, Bohse J, Hinrichsen G (1999) Composites A 30:747
20. Kelly G, Hallstrom S (2005) Compos Struct 69:301
21. Kaynak C, Orgun O, Tincer T (2005) Polym Test 24:455
22. Meraghni F, Blakeman CJ, Benzeggagh ML (1996) Compos Sci Technol 56:541
23. Naganuma T, Naito K, Kyono J, Kagawa Y (2009) Compos Sci Technol 69:2428
24. Gourichon B, Binetruy C, Krawczak P (2006) Composites A 37:1961
25. Czigany T, Poloskei K, Karger-Kocsis J (2005) J Mater Sci 40:5609. doi:10.1007/s10853-005-1273-8
26. Nath RB, Fenner DN, Galiotis C (2000) Composites A 31:929
27. Barre S, Chotard T, Benzeggagh ML (1996) Composites A 27:1169